Commun Nonlinear Sci Numer Simulat 22 (2015) 641–649

Contents lists available at ScienceDirect

Commun Nonlinear Sci Numer Simulat

journal homepage: www.elsevier.com/locate/cnsns

Ghost stochastic resonance induced by a power-law distributed noise in the FitzHugh–Nagumo neuron model

Iacyel G. Silva [a], Osvaldo A. Rosso [a,b,c], Marcos V.D. Vermelho [a], Marcelo L. Lyra [a,*]

[a] Instituto de Física, Universidade Federal de Alagoas, 57072-970 Maceió, AL, Brazil
[b] LaCCAN/CPMAT – Instituto de Computação, Universidade Federal de Alagoas, 57072-970 Maceió, AL, Brazil
[c] Instituto Tecnológico Buenos Aires (ITBA), Buenos Aires, Argentina

ARTICLE INFO

Article history:
Received 11 April 2014
Received in revised form 23 June 2014
Accepted 30 June 2014
Available online 7 August 2014

Keywords:
Stochastic resonance
Ghost resonance
Power-law noise
Neuron model

ABSTRACT

We numerically investigate the ghost stochastic resonance phenomenon induced by a power-law distributed noise in the neuron FitzHugh–Nagumo model. The input noise considered is produced by a Langevin process including both multiplicative and additive Gaussian noise sources. In this process, the power-law decay exponent of the resulting noise distribution is governed by the off-set of the multiplicative noise, thus allowing us to probe both regimes of Gaussian and strongly non-Gaussian noises. Ghost stochastic resonance, i.e., stochastic resonance in a missing fundamental harmonic, occurs in this model. Deviations from the Gaussianity of the input noise are shown to reduce both the additive noise intensity corresponding to the optimal identification of the missing fundamental as well as the number of firing events at the ghost stochastic resonance condition.

1. Introduction

The influence of noise on the time evolution of dynamical systems is quite diverse. Besides its standard effect of producing disorder and, therefore, compromising the identification of a regular input signal, it can have the opposite effect of improving the system's response to an external stimulus under appropriated conditions. In particular, the study of neural systems under the influence of a noise source is fundamental to fully understand its dynamics. For example, neurons in vitro fire with considerable regularity in response to a constant stimulus while neurons in vivo exhibit a much larger irregularity in response to the same stimulus. A number of possible sources for neuronal noise in vivo has been proposed, including an intrinsic channel [1], Johnson electrical [2] and network [3] noises. Among the many positive roles played by noise in dynamical systems, the stochastic resonance (SR) phenomenon is one of the most intriguing. SR is the optimal detection of a sinusoidal sub-threshold signal achieved at a characteristic noise level. Along the years, SR has contributed to change the traditional concept of noise as a disturbing agent [4–15].

Recently, SR has been used to explain a phenomenon that happens in the human ear known as the "missing fundamental illusion". In this phenomenology, the human ear can perceive tones that are not present in the characteristic function of pressed notes [16–19]. This phenomenon has been studied in a model of neurons and compared with the general case of unharmonious tones used in the experiments of Schouten [20] where the complex signal was constructed adding pure high-order harmonics of a fundamental frequency. Ghost resonance produced by noise was observed with good agreement

* Corresponding author.
E-mail addresses: ciel33@yahoo.com (I.G. Silva), oarosso@gmail.com (O.A. Rosso), vermelho@fis.ufal.br (M.V.D. Vermelho), marcelo@fis.ufal.br (M.L. Lyra).

http://dx.doi.org/10.1016/j.cnsns.2014.06.050
1007-5704/

with experiments. The missing frequency resonance phenomenon promoted by noise has been termed as *ghost stochastic resonance* (GSR) and it has been detected in different systems like lasers [21], electronic circuits [22] and chaotic systems [23].

Usually, GSR frequency is investigated when a given dynamical system is driven by a white Gaussian noise source. However, non-Gaussian noises are quite frequent in biological systems. For example, some experimental results in sensory systems, particularly for one kind of crayfish, as well as in rat skin experiments, offer strong indications that the noise source in these systems could be non-Gaussian [24]. Experimental studies in rat sensory neurons have demonstrated that, under certain circumstances, colored noise can be better than white Gaussian noise for enhancing the neuron response to a weak signal [25]. Although several studies have addressed the question of the influence of the noise statistical properties on the stochastic identification of weak harmonic signals [26], there still lacks a better understanding of how the noise characteristics can affect the missing fundamental illusion in sensory neuron models.

In the present work, we investigate how the noise deviation from Gaussianity influences the GSR characteristics exhibited by a nonlinear sub-threshold dynamical system. As a prototype model, we will consider the FitzHugh–Nagumo (FHN) neural model driven by superposed harmonics of a missing fundamental and a power-law distributed noise source resulting from a Langevin process including both additive and multiplicative Gaussian noises. By controlling the model parameters, one can tune the degree of deviation from Gaussianity and explore its influence on the characteristic noise intensity leading to an optimal identification of the missing fundamental.

This work is organized as follows: In Section 2, we review some basic aspects of stochastic and ghost resonances. In Section 3, we describe the main features of the FitzHugh–Nagumo neural model. The Langevin process leading to the production of a power-law distributed noise is detailed in Section 4. Section 5 is devoted to the numerical methodology we used and to the main results characterizing the GSR phenomenon in the modeled system. Finally, we summarize and draw our main conclusions in Section 6.

2. Stochastic and ghost resonances

When a nonlinear dynamical system is driven by a sub-threshold periodical signal, the superposition of an input noise can make the output signal to bring information regarding the external sub-threshold input. Usually there is an optimal intensity of the superposed noise that leads to the highest resolution of the sub-threshold periodic signal. This effect is known as SR and it has been studied in several different physical scenarios such as lasers, chemical reactions, and chaotic systems [27–29].

The ghost resonance is a variant of the SR phenomenon in which the periodic stimulus is a superposition of higher harmonics, equally spaced in frequency, of a fundamental tone [16–23]. When the maximum of this complex signal is sub-threshold, a SR condition can be reached in the presence of noise. However, the main SR is not in any of the frequencies contained in the periodic stimulus but rather in the missing fundamental tone. This phenomenon is referred as the missing fundamental illusion, or in this case, GSR because the perceived tone corresponds to the fundamental frequency for which there is no actual source. It only appears in the output signal due to the presence of noise. This phenomenon has been shown to be directly related to pitch perception of complex sound waves [17]. Within this context, a relevant question refers to the shift in the pitch perception when the frequencies of the harmonic tones are rigidly displaced, which makes them no longer higher harmonics of a fundamental tone. The external complex stimulus is usually considered as a superposition of sinusoidal functions in the form

$$F(t) = A\{sin(2\pi f_1 t) + sin(2\pi f_2 t) + \cdots + sin(2\pi f_n t)\} \tag{1}$$

where $f_1 = kf_0 + \Delta f; f_2 = (k+1)f_0 + \Delta f; \ldots; f_n = (k+n-1)f_0 + \Delta f$. Here, Δf is a frequency shift from a perfect harmonic series, f_0 is the fundamental tone, and A is the amplitude of the signal components. A SR is observed in frequencies given by Ref. [18,19]

$$f_r = f_0 + \Delta f/[k + (n-1)/2], \tag{2}$$

where $n = 1, 2, 3, \ldots$ and $k > 1$. The above equation actually corresponds to the expected frequency at which the highest peaks of the complex signal occur. Such prediction has been probed in several physical systems such as the neuron model [18], semiconductor lasers [22], chaotic systems [23] and electronic circuits [21,23]. It has also been well reproduced in experiments of pitch perception [20]. A recent review on GSR and its different manifestations can be found in Ref. [16].

3. The FitzHugh–Nagumo neuron model

The FitzHugh–Nagumo neuron (FHN) model is a representative example of a bistable excitable system that occurs in a wide range of applications ranging from kinetics of chemical reactions to biological processes. Different aspects of the dynamics of this model and similar excitable ones in the presence of noise have been discussed from different points of view [30–34]. The equation of motion for the FHN neuron is given by

$$\begin{cases} \epsilon \frac{dv}{dt} = v(v-a)(1-v) - \omega + F(t) + v(t) \\ \frac{d\omega}{dt} = v - \omega - b \end{cases} \tag{3}$$

where $v(t)$ is a fast variable representing a dimensionless membrane voltage and $\omega(t)$ is a slow variable with a unitary characteristic time constant. The time constant ϵ governs the speed of changes in the fast variable $v(t)$ in comparison to the slow variable $\omega(t)$. It will be fixed at $\epsilon = 0.002$ s in the following numerical study. The parameter a accounts for an unstable fixed point and b for the resting voltage. These will be considered to assume the values $a = 0.5$, and $b = 0.15$ which reproduce a typical neuron firing sequence. The sum $F(t) + v(t)$ is an external stimulus given by a combination of periodic force [see Eq. (2)] and the noise component. When the intensity of the stimulus is fixed below threshold, no firing can be observed in $v(t)$. Increasing the intensity of the stimulus, a firing recovery produces an absolute refractory time T_R during which a second firing cannot occur, followed by a longer relative refractory time during which firing requires stronger perturbations. Thus, the firing threshold depends on the time interval since the previous firing. In Fig. 1, we show a typical time evolution of the system fast voltage $v(t)$ under the influence of an external stimulus. The time at which spikes appear are denoted by t_i. In consequence, the inter-spike intervals (ISI) are given by $\Delta t_i = t_i - t_{i-1}$.

4. Power-law distributed noise and its numerical generation

In the present work, we will consider the noise input $v(t)$ to be power-law distributed. In order to numerically generate such class of noises, we employed a Langevin differential stochastic process including both additive and multiplicative underlying noise sources governed by the following equation [35–37].

$$\frac{dv(t)}{dt} = \lambda(t)v(t) + \xi(t), \tag{4}$$

where $v(t)$ is the stochastic variable to be used as the input noise in the neuron system, $\lambda(t)$ is a multiplicative noise and $\xi(t)$ an additive noise. A unitary characteristic time scale is assumed. Both $\lambda(t)$ and $\xi(t)$ are white and Gaussian, with average and variance given by

$$\begin{aligned} &\langle\lambda(t)\rangle = \lambda_0 < 0, \\ &\langle(\lambda(t) - \lambda_0)(\lambda(t') - \lambda_0)\rangle = 2D_\lambda\delta(t - t'), \\ &\langle\xi(t)\rangle = 0, \\ &\langle\xi(t)\xi(t')\rangle = 2D_\xi\delta(t - t\prime). \end{aligned} \tag{5}$$

In the above equations D_λ and D_ξ are the multiplicative and additive noises fluctuation intensities, and λ_0 is a constant offset of the multiplicative noise.

In most practical situations, the additive noise is weaker than the multiplicative noise. In analog simulations of the above process, for example, the additive noise is just produced by small thermal noises of operational amplifiers or from external electromagnetic noises. In a detailed analytical study of this stochastic process, it has been shown that the Fokker–Planck equation satisfied by the probability distribution function $P(v;t)$ of $v(t)$ is given by

$$\frac{\partial P}{\partial t} = -\frac{\partial}{\partial v}\left[(\lambda_0 + D_\lambda)vP - \frac{\partial}{\partial v}[(D_\lambda v^2 + D_\xi)P]\right], \tag{6}$$

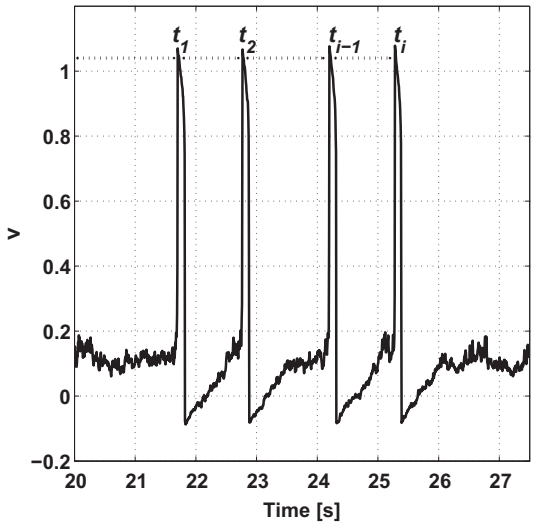

Fig. 1. Typical time evolution of the neuron system output $v(t)$ under the influence of an external signal $F(t) + v(t)$.We denoted by t_i the time at which a spike is observed.

which has as stationary solution

$$P(v) \propto \left[1 + \left(\frac{v^2}{s}\right)\right]^{-(\beta+1)/2}, \tag{7}$$

with $s = \sqrt{D_\xi/D_\lambda}$ and $\beta = -\lambda_0/D_\lambda$. The strength of the generated noise can be characterized by its variance

$$2D_v = \langle v^2 \rangle = \frac{2D_\xi}{D_\lambda(\beta - 2)}. \tag{8}$$

Boundary conditions with no probability flux were assumed to produce stationarity. The weak additive noise condition implies $s \ll 1$. Therefore the stochastic signal has an asymptotic power-law distribution $P(v/s \gg 1) \propto (v/s)^{-(\beta+1)}$. Observe that the characteristic power-law exponent β is determined only by statistical characteristics of the multiplicative noise. Thus, the average multiplicative noise λ_0 will be used in this work to tune the power-law distribution exponent. In what follows, we will work in units of $D_{\lambda=1}$. Therefore, D_ξ will measure the fluctuations on the additive noise relative to those on the multiplicative noise, which ultimately determine the characteristic scale s of the power-law generated noise. Therefore, by changing the pair of parameters (λ, D_{eta}), one can fully tune the statistical properties of the noise that is going to be superposed to the complex periodic signal feeding the FitzHugh–Nagumo neuron model. A detailed study of this stochastic process, Eq. (4), can be found in references [35–37].

To numerically integrate the power-law noise equation, we rewrote Eq. (4) in order to use the Euler numerical integration method. We defined $\lambda(t) = N(t) + \lambda_0$, where $N(t)$ is a white noise that has the same characteristics of $\xi(t)$ and fluctuation intensity D_λ. Using this relation, one can rewrite Eq. (4) as

$$dv(t) = \lambda_0 v(t)dt + N(t)v(t)dt + \xi(t)dt. \tag{9}$$

Using Ito and Stratonovich theory for integrating stochastic differential equations [36], we can write Eq. (9) in the form

$$dv(t) = \lambda_0 v(t)dt + v(t)dN' + 0.5v(t)(dN')^2 + dW, \tag{10}$$

where $dN' = N(t)dt$ and $dW = \xi(t)dt$ represent Wiener process increments. According to the central limit theorem, dN' and dW have Gaussian distributions with variance $2D_\lambda dt$ and $2D_\xi dt$, respectively. Therefore, during the numerical integration, the Wiener increments were generated by $\Delta N' = R_G\sqrt{2D_\lambda dt}$ and, $\Delta W = R_G\sqrt{2D_\xi dt}$, where the values of R_G were taken, at each time increment, as random uncorrelated numbers sampled from a Gaussian distribution with unitary variance. For the multiplicative noise, the quadratic term in the Wiener increment was included to improve the convergence, according to Stratonovich's prescription. It effectively takes the average of the values at the beginning and at the end of the integration interval dt as a better approximation of $v(t)$.

As an example, we show some distribution functions for the resulting noise in Fig. 2, characterized by distinct values of the parameter λ_0 and the intensity of the additive noise D_ξ. In the first case, we took $\lambda_0 = -2.5, D_\xi = 0.001$ (black asterisk)

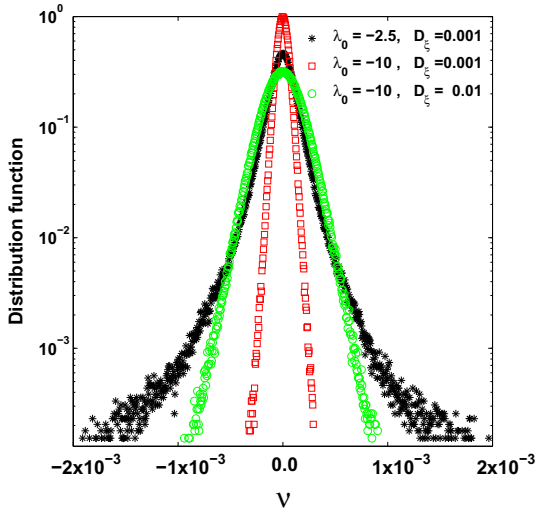

Fig. 2. Distribution functions for the noise $v(t)$ generated using distinct sets of the parameters λ_0 and D_ξ. The power-law decay exponent of the distribution is controlled by the value of λ_0. A typical noise with a slow power-law decay (long-tailed distribution) is shown for $\lambda_0 = -2.5$ and $D_\xi = 0.001$ (black asterisk). Nearly Gaussian noises with distinct variances are produced for $\lambda_0 = -10$, with $D_\xi = 0.001$ (red square) and, $D_\xi = 0.01$ (green circle). (For interpretation of the references to colour in this figure caption, the reader is referred to the web version of this article.)

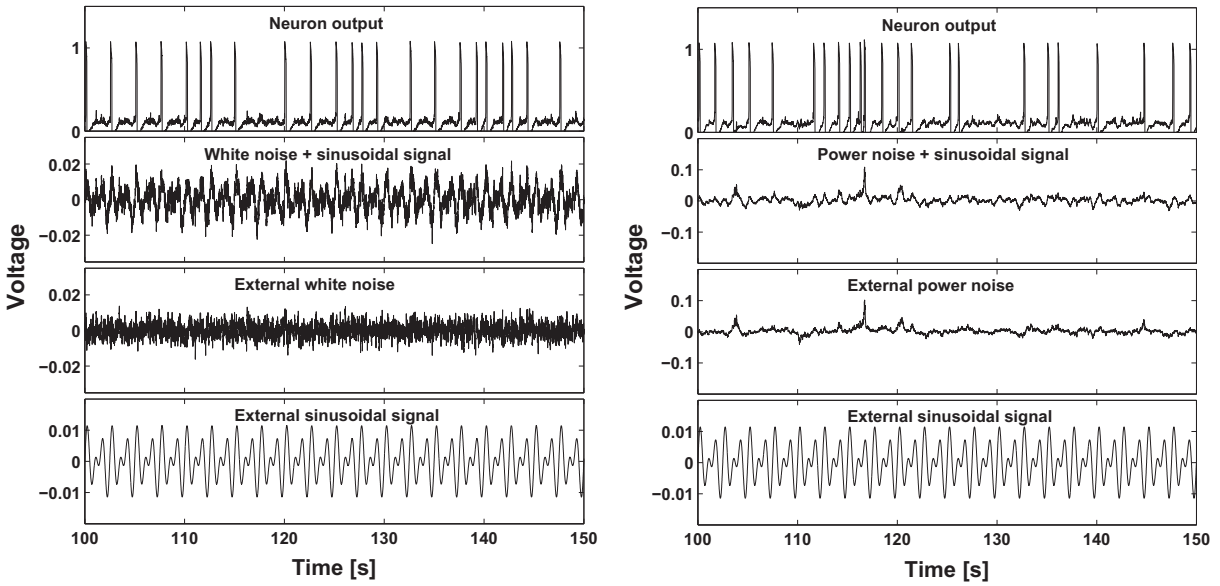

Fig. 3. Typical time series of the underlying complex periodic signal, noise, superposed signal and noise, and neuron voltage. The cases of a nearly Gaussian ($\lambda_0 = -40$) and strongly nongaussian ($\lambda_0 = -2.5$) noises are illustrated. Notice that, under the presence of a nongaussian noise, the neuron input signal has a broader distribution and the neuron firings are more correlated to the occurrence of large noise events.

which represent a typical noise with a slow power-law decay (long-tailed distribution). For the second and third cases, we consider $\lambda_0 = -10, D_\xi = 0.001$ (red square) and $\lambda_0 = -10, D_\xi = 0.01$ (green circle) where almost Gaussian noises are produced. In our numerical simulations, we fixed $dt = 10^{-4}$ s and $D_\lambda = 1$. In the following study of the neural dynamics under the influence of a power-law distributed noise, the corresponding values of λ_0 and D_ξ will be adjusted to detect the GSR.

5. Methodology and results

For the numerical resolution of the nonlinear equation (3), we used a simple Euler method with an integration step of 0.0001 s. The total number of points used in our simulation was $5 \cdot 10^7$ and we saved one point at each 50 steps of integration. The following density plots were obtained by computing the histograms of the typical frequencies of firing events $f_j = 1/(t_j - t_{j-1})$ in the output signal $v(t)$ (inter-spikes time intervals (ISI), see Fig. 1). The histograms were evaluated by counting the number of occurrences of f_j within a window of 0.01 Hz. The methodology presented here was used to produce all numerical results.

In Fig. 3 we report comparative time series of the neuron signal together with the complex periodic signal superposed with nearly Gaussian ($\lambda_0 = -40$) as well as strongly nongaussian ($\lambda_0 = -2.5$) noises. Notice that, due to the long tail character of the nongaussian noise distribution, the resulting noisy input signal has a broader distribution of intensities when compared to the case of a Gaussian noise. Under the presence of a nongaussian noise, the neuron firings are more correlated to the occurrence of large noise events than to the peaks of the periodic complex signal. This feature can have an impact on the stochastic identification of the underlying weak complex signal, which will be explored in the following.

The methodology utilized to detect the GSR is described in different works, and can be summarized in two steps. In the first step, one fixes the intensity of the external periodical signal below threshold. After that, we add the noise and change its intensity. With this procedure, one searches for the optimal noise intensity that produces a maximum output response on the resonance frequency. This is actually the typical procedure to find the optimal noise in the SR case. In a second step, we fixed the noise at this optimal level and vary Δf to find the general characteristic of the ghost stochastic resonance predicted by Eq. (2) [16,19,21–23].

5.1. Ghost stochastic resonance: Gaussian noise results

Following the above procedure, we were able to build Fig. 4, for which we have set $\lambda_0 = -40$, $D_\lambda = 1, f = 0.4$ Hz, $\Delta f = 0$, $n = 2, k = 2, A = 6.0 \times 10^{-3}$ and distinct levels of the additive noise intensity $D_\xi = (100, 600, 750, 1400) \times 10^{-6}$. In this case of large multiplicative noise intensity $\lambda_0 = -40$, the resulting noise feeding the neural model has an almost Gaussian distribution. Notice the signatures of SR in Fig. 4. There is an optimal detection of the external sub-harmonic signal frequency $f_0 = 0.4$ Hz at an additive noise intensity $D_\xi = 600 \times 10^{-6}$. That is, for this noise level, the number of events (histogram)

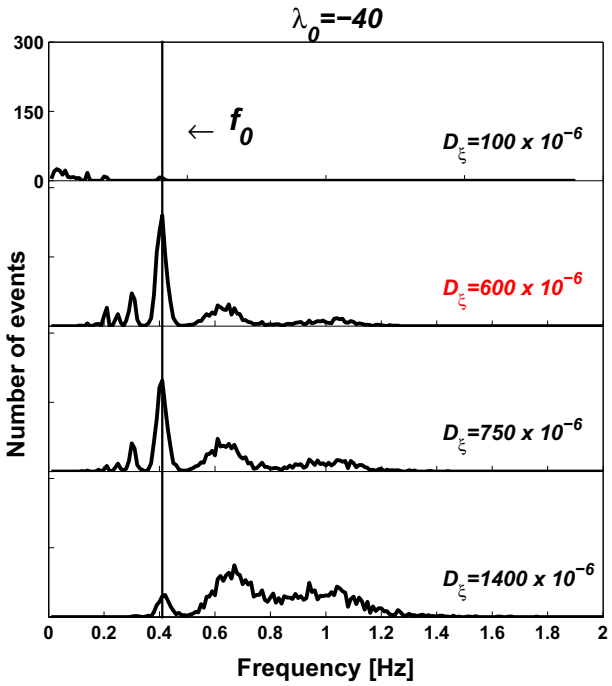

Fig. 4. Distribution function of the number of events versus the frequency response of the system output $v(t)$ (amplitude histogram), for different values of $D_\xi = (100, 600, 750, 1400) \times 10^{-6}$. We have set $\lambda_0 = -40, D_\lambda = 1, n = 2, f_1 = 0.8$ Hz, $f_2 = 1.2$ Hz ($f_0 = f_2 - f_1 = 0.4$ Hz), $A = 6.0 \times 10^{-3}$. Note that the ghost resonance appears at the missing fundamental frequency (corresponding to the case of $\Delta_f = 0$ and $k = 2$ in Eq. (2)) as a maximum number of events when the system is driven by an optimal additive noise intensity $D_\xi = 600 \times 10^{-6}$. After that, this peak slowly degrades, in agreement with the general theory. The axis are on the same scale in all the graphs. Notice that a few other maxima at lower frequencies are also identifiable at the optimal condition. These correspond roughly to the resonance frequencies predicted by Eq. (2) for the cases of $k = 3$ (for which $\Delta f = -0.4$ and $f_r = 0.285$), $k = 4$ (for which $\Delta f = -0.8$ and $f_r = 0.22$), and $k = 5$ (for which $\Delta f = -1.2$ and $f_r = 0.22$).

is maximized at frequency $f_0 = 0.4$ Hz in comparison with the other maxima. Due to fact that $f_0 = 0.4$ Hz is not present in the external sinusoidal signal, this phenomenon is also the signature of ghost stochastic resonance. Notice that a few other maxima at lower frequencies are also identifiable at the optimal condition. These correspond to the resonance frequencies predicted by Eq. (2) for the cases of $k = 3$ (for which $\Delta f = -0.4$ and $f_r = 0.285$), $k = 4$ (for which $\Delta f = -0.8$ and $f_r = 0.22$), and $k = 5$ (for which $\Delta f = -1.2$ and $f_r = 0.22$).

To observe the general characteristic of the GSR effect, we set the system in the parameters utilized in the above numerical experiment, i.e., we fixed the system at the optimal additive noise intensity $D_\xi = 600 \times 10^{-6}$, and varied the frequency shift in the range -0.6 Hz $\leqslant \Delta f \leqslant 0.6$ Hz with displacements of 0.1 Hz. The obtained results are shown in Fig. 5. The general configuration of ghost frequency appears according to the theory prediction Eq. (2). In this figure, the red line signals the fundamental frequency. The transverse lines correspond to the theoretical prediction for the location of the resonance frequency (see Eq. (2)), for the cases of $k = 1, 2, 3$ and 4.

5.2. Ghost stochastic resonance: power-law distributed noise

The same procedure used in the previous subsection for the case of a Gaussian-like noise was employed for the case of a power-law distributed noise. In Fig. 6, we show the distribution of the number of events when $\lambda_0 = -2.5$, which corresponds to a slow decay of the noise distribution that stimulates the neuron model, and different levels of the additive noise $D_\xi = (50, 120, 250, 750) \times 10^{-6}$. Note that GSR also appears when the external noise has a slowly decaying power-law tail. In this case, the optimal additive noise intensity corresponding to the maximum signal of the missing fundamental is weaker than the one achieved for a Gaussian-like noise. In Fig. 7, we show the general configuration of the GSR when the system is stimulated by such optimal additive noise intensity $D_\xi = 120 \times 10^{-6}$. It is worth to call attention to the fact that the number of firing events at the resonance condition is smaller than the one attained under the influence of a Gaussian noise. As a consequence, the poorer statistics compromises the clear identification of the other lower frequency resonances.

Before finishing, we report in Fig. 8 the full dependence of the amplitude of the response (histogram value) at the missing fundamental frequency as a function of λ_0 and D_ξ. Values are normalized to the maximum response for better visualization.

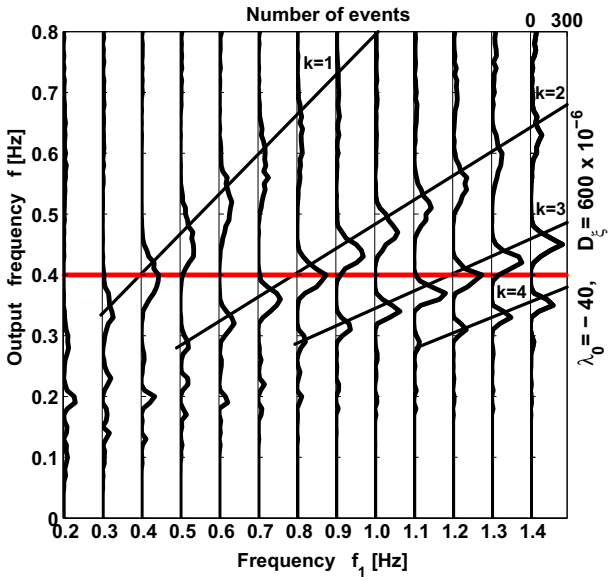

Fig. 5. Distribution function of the number of events versus the frequency response of system output $v(t)$ (amplitude histogram) for distinct values of the frequency f_1 for the case of a complex sub-threshold input periodic signal. Model parameters are $\lambda_0 = -40$ (Gaussian-like distribution), $D_\lambda = 1, f_0 = 0.4\,\text{Hz}, D_\xi = 600 \times 10^{-6}$ (optimal additive noise intensity), $n = 2, k = 2, A = 6.0 \times 10^{-3}$. The red line signals the fundamental frequency. The transverse lines represent the theoretical prediction for the location of the resonance frequencies (see Eq. (2)).

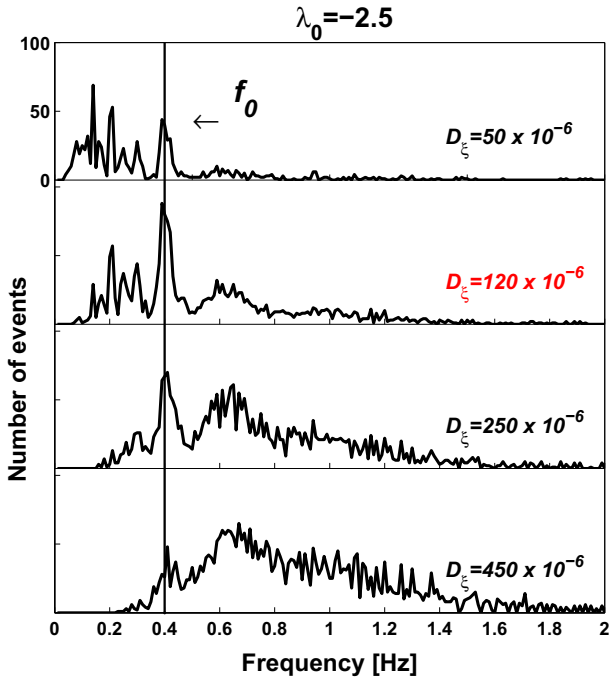

Fig. 6. Distribution function of the number of events versus the frequency response of the system output $v(t)$ (amplitude histogram), for different values of $D_\xi = (50, 120, 250, 450) \times 10^{-6}$. We have set $\lambda_0 = -2.5, D_\lambda = 1, n = 2, k = 2, A = 6.0 \times 10^{-3}, f_0 = 0.4\,\text{Hz}, \Delta f = 0$. The optimal identification of the missing fundamental appears at the additive noise intensity $D_\xi = 120 \times 10^{-6}$.Axis scale is the same on all graphs.

Besides clearly showing that the optimal noise intensity decreases as one further deviates from gaussianity (smaller values of λ_0), Fig. 8 unveils that the GSR condition becomes sharper. Therefore, while a weaker noise intensity is required to identify the missing fundamental frequency under the influence of a nongaussian noise, its resolution appears in a narrower range of noise intensities.

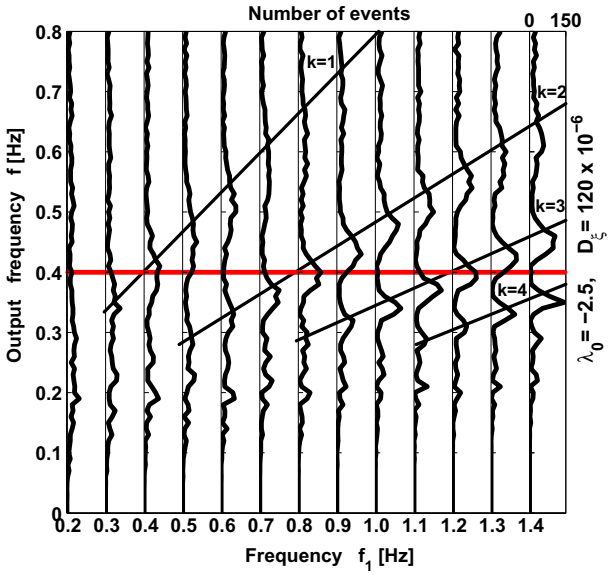

Fig. 7. Distribution function of the number of events versus the frequency response of the system output $v(t)$ (amplitude histogram) for distinct values of the frequency f_1 for the case of a complex sub-threshold input periodic signal. Model parameters are $\lambda_0 = -2.5$ (slowly decaying power-law distributed noise), $D_\lambda = 1, f_0 = 0.4$ Hz, $D_\xi = 120 \times 10^{-6}$ (optimal additive noise intensity), $n = 2, k = 2, A = 6.0 \times 10^{-3}$. The red line signals the fundamental frequency. The transverse lines represent the theoretical prediction for the location of the resonance frequencies (see Eq. (2)). (For interpretation of the references to colour in this figure caption, the reader is referred to the web version of this article.)

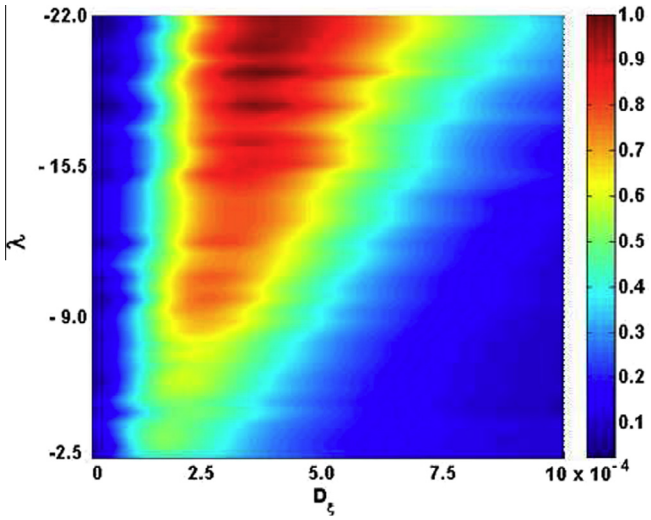

Fig. 8. Color plot of the response at the missing fundamental frequency (normalized histogram values) as a function of λ_0 and D_ξ. Data were normalized to the maximum response for better visualization. Notice that, while weaker intensities of the additive noise D_ξ are required to reach the resonance condition as one further deviates from gaussianity (smaller values of λ_0), the resonance condition becomes sharper. (For interpretation of the references to colour in this figure caption, the reader is referred to the web version of this article.)

6. Summary and conclusions

In summary, we investigated the occurrence of the GSR phenomenon on the FitzHugh–Nagumo neural model under the influence of a power-law distributed noise. Such noise results from a Langevin process including both additive and multiplicative Gaussian noises. When the noise signal is superposed to a sub-threshold periodic stimulus composed of a linear combination of high harmonics of a fundamental tone, the histogram of the firing events of the system presents a pronounced peak at the missing fundamental frequency. For fixed statistical properties of the multiplicative noise, mainly its average and variance, we observed that the optimal identification of the missing fundamental tone is achieved at an intermediate value of the additive noise intensity which decreases as the input power-law noise deviates further from Gaussianity. Further, a smaller number of firing events occurs at the GSR condition when considering a non-Gaussian noise input.

The above two features related to the influence of noise non-Gaussianity on the GSR phenomenon can be better understood by stressing that the intensity of the input power-law noise (see Eq. (8)) is proportional to the additive noise intensity D_ξ and decreases with increasing values of the average multiplicative noise $(-\lambda_0)$. Therefore, when $(-\lambda_0)$ is decreased to enhance the non-Gaussian character of the input noise, a smaller intensity of the additive noise is required to produce the same input noise intensity. As a consequence, the number of firing events decreases because the rare events of large noise intensities have a mayor influence on the process. Considering that the neural response is quite sensitive to the noise statistical properties [38,39] and that non-Gaussian noise are commonly found in nature [40], the present results sheds new light on the possible mechanisms explored by biological dynamical systems, specially the auditory system, to identify hidden fundamental harmonics in low intensity complex signals.

Acknowledgments

We acknowledge support from the Brazilian research agencies CAPES, CNPq and FINEP, as well as from the Alagoas state research agency FAPEAL. O.A. Rosso also gratefully acknowledges support from CONICET.

References

[1] Mainen ZF, Sejnowski TJ. Science 1995;268:1503.
[2] White JA, Rubinstein JT, Kay AR. Trends Neurosci 2000;23:131.
[3] Durran S, Kang Y, Socks N, Feng J. Phys Rev E 2011;84:011923.
[4] Macnamara B, Weisenfeld K. Phys Rev A 1989;39:4854.
[5] Jung P, Hanggi P. Phys Rev A 1991;44:8032.
[6] Bulsara A, Hanggi P, Marchesoni F, Moss F, Shlesinger M. J Stat Phys 1993;70:1.
[7] Weisenfeld K, Moss F. Nature 1995;73:33.
[8] Gammaitoni L, Hänggi P, Jung P, Marchesoni F. Rev Mod Phys 1998;70:223.
[9] Hanggi P. Chem Phys Chem 2002;3:285.
[10] Guo Y, Tan J. Commun Nonlinear Sci Numer Simul 2013;18:2852.
[11] Liu C, Wang J, Yu HT, Deng B, Tsang KM, Chan WL, Wong YK. Commun Nonlinear Sci Numer Simul 2013;19:1088.
[12] Yilmaz E, Uzuntarla M, Ozer M, Perc M. Physica A 2013;392:5735.
[13] Koverda VP, Skokov VN. Physica A 2014;393:173.
[14] Kohar V, Murali K, Sinha S. Commun Nonlinear Sci Numer Simul 2014;19:2866.
[15] Turutanov OG, Golovanevskiy VA, Lyakhno VY, Shnyrkov VI. Physica A 2014;396:1.
[16] Balenzuela P, Braun H, Chialvo DR. Contemp Phys 2012;53:17.
[17] Ushakov YV, Dubkov A, Spagnolo B. Phys Rev E 2010;81.
[18] Chialvo DR, Calvo O, Gonzalez DL, Piro O, Savino GV. Phys Rev E 2002;65:050902R.
[19] Chialvo DR. Chaos 2003;13:1226.
[20] Schouten JF, Ritsma RJ, Lopes Cardozo B. J Acoust Soc Am 1962;34:1418.
[21] Calvo O, Chialvo DR. Int J Bifurcation Chaos 2006;16:731.
[22] Buldu JM, Chialvo DR, Mirasso CR, Torrent MC, Garcia-Ojalvo J. Europhys Lett 2003;64:178.
[23] Gomes I, Vermelho MVD, Lyra ML. Phys Rev E 2012;85:056201.
[24] Castro FJ, Kuperman MN, Fuentes M, Wio HS. Phys Rev E 2001;64:051105.
[25] Nozaki D, Mar DJ, Grigg P, Collins JJ. Phys Rev Lett 1999;82:2402.
[26] See, e.g. Wio H. On the role of non-Gaussian noises on noise-induced phenomena. In: Gell-Mann Murray, Tsallis Constantino, editors. Nonextensive Entropy: Interdisciplinary Applications. New York: Oxford University Press; 2004. and references therein.
[27] Singh KP, Sinha S. Phys Rev E 2011;83:046219.
[28] Dauxois T, Di Patti F, Fanelli D, McKane AJ. Phys Rev E 2009;79:036112.
[29] Korneta W, Gomes I, Mirasso CR, Toral R, Calvo O. Physica D 2006;219:93.
[30] Lindner B, Garcia-Ojalvo J, Neiman A, Schimansky-Geier L. Phys Rep 2004;392:321.
[31] Alarcón T, Perez-Madrid A, Rubí JM. Phys Rev E 1998;57:4979.
[32] Lee S, Shin CW, Kim S. J Korean Phys Soc 2006;48:S192.
[33] Zeng CH, Zeng CP, Gong AL, Nie LR. Physica A 2010;389:5117.
[34] Bemmo DT, Siewe MS, Tchawoua C. Commun Nonlinear Sci Numer Simul 2014;18:1275.
[35] Duarte JRR, Lyra ML. Int J Mod Phys C 2010;21:757.
[36] Gardiner CW. Handbook of stochastic methods: for physics, chemistry and the natural sciences. Berlin: Springer-Verlag; 1999.
[37] Silva LBM, Vermelho MVD, Lyra ML, Viswanathan GM. Chaos Solitons Fract 2009;41:2806.
[38] Nozaki D, Yamamoto Y. Phys Lett A 1998;243:281.
[39] Nozaki D, Mar DJ, Grigg P, Collins JJ. Phys Rev Lett 1999;82:2402.
[40] Newman MEJ. Contemp Phys 2005;46:323.